Journal of Cell Science 108, 2993-3002 (1995)
Printed in Great Britain © The Company of Biologists Limited 1995

Localization of MIWC and GLIP water channel homologs in neuromuscular, epithelial and glandular tissues

Antonio Frigeri[1], Michael A. Gropper[1], Fuminori Umenishi[1], M. Kawashima[2], Dennis Brown[2] and A. S. Verkman[1,*]

[1]Departments of Medicine, Physiology and Anesthesia, Cardiovascular Research Institute, University of California, San Francisco, CA 94143-0521, USA
[2]Renal Unit, Massachusetts General Hospital, Boston, MA 02114, USA

*Author for correspondence

SUMMARY

It was shown recently that water channel homologs MIWC (mercurial insensitive water channel) and GLIP (glycerol intrinsic protein) colocalized in basolateral membranes of kidney collecting duct, tracheal and colonic epithelia, and in brain pia mater. We report here an extensive immunolocalization study of MIWC and GLIP in non-epithelial and glandular epithelial tissues in rat. Immunogold electron microscopy confirmed colocalization of MIWC and GLIP in basolateral membrane of principal cells in kidney collecting duct. However, in other epithelia, MIWC but not GLIP was expressed in basolateral membrane of parietal cells in stomach, and in excretory tubules of salivary and lacrimal glands; GLIP but not MIWC was expressed in transitional epithelium of urinary bladder and skin epidermis. In the central nervous system, MIWC was strongly expressed in the ependymal layer lining the aqueductal system, and in astrocytes throughout the spinal cord and in selected regions of brain. MIWC was also expressed in a plasma membrane pattern in skeletal, but not smooth or cardiac muscle. Neither protein was expressed in small intestine, testis, liver, spleen and nerve. The tissue-specific expression of MIWC suggests a role in fluid transport and/or cell volume regulation in stomach and glandular epithelia. The functional role of MIWC expression in the neuromuscular system and of GLIP expression in skin and urinary bladder is uncertain. The specific cellular sites of MIWC expression (astrocytes, trachea, sarcolemma, gastric parietal cells and kidney principal cells) correspond exactly to sites where orthogonal arrays of particles (OAPs) have been visualized by freeze-fracture electron microscopy, suggesting that MIWC may be the OAP protein.

Key words: water transport, mercurial-insensitive water channel, GLIP, immunolocalization, aquaporin

INTRODUCTION

A family of related water transporting proteins (aquaporins) expressed in mammalian tissues has been identified recently. The first such protein was CHIP28 (Preston et al., 1991), a small hydrophobic protein that forms selective water channel when expressed in *Xenopus* oocytes (Preston et al., 1992; Zhang et al., 1993) and mammalian cells (Ma et al., 1993b), or when reconstituted into proteoliposomes (Van Hoek and Verkman, 1992). CHIP28 is expressed widely in various epithelia and capillary endothelia, including proximal tubule and thin descending limb in kidney (Sabolic et al., 1992; Hasegawa et al., 1993, 1994a; Nielsen et al., 1993ab; Bondy et al., 1993). A second water channel expressed selectively in kidney collecting duct apical membrane was identified (Fushimi et al., 1993), which was proven to be the vasopressin-inducible water channel by its mutation in congenital nephrogenic diabetes insipidus (Deen et al., 1994) and its vasopressin-dependent membrane targeting (DiGiovanni et al., 1994; Sabolic et al., 1995). A third family member, MIWC, was the first mercurial-insensitive water channel identified (Hasegawa et al., 1994b) and was expressed in multiple tissues, including the basolateral membrane of kidney collecting duct (Frigeri et al., 1995). An unusual feature of MIWC was the tissue-specific expression of a spliced transcript in which exon 2 was deleted. Recently, another family member given the names GLIP (glycerol intrinsic protein) and AQP-3 was cloned by 3 laboratories (Ishibashi et al., 1994; Ma et al., 1994; Echavarria et al., 1994). Initial immunolocalization studies indicated expression in basolateral membrane of kidney collecting duct (Ishibashi et al., 1994; Ma et al., 1994); all groups reported that GLIP (AQP-3) transported glycerol when expressed in *Xenopus* oocytes; however, our laboratory (Ma et al., 1994) found little or no increase in osmotic water permeability. Recently, another related water transporting protein (AQP-5; Raina et al., 1995) was identified with expression in salivary gland, lacrimal gland and lung. These proteins are members of the MIP superfamily of small 'channel-forming' proteins (Reizer et al., 1993; Verkman, 1993) which include proteins from plants, bacteria, *Drosophila* and yeast. An initial immunolocalization study focusing on epithelial tissues demonstrated that MIWC and GLIP proteins were coexpressed

on the same plasma membrane in several tissues, including basolateral membrane of principal cells in kidney collecting duct, basolateral membrane of tracheal and colonic villus epithelium, and ependymal/meningeal cells lining the ventricles and surface of brain (Frigeri et al., 1995). In addition, expression of MIWC but not GLIP was reported in lung (in bronchial epithelium), and eye (in ciliary body epithelium) and the nuclear layer of retina. These studies suggested a role for MIWC and GLIP in the urinary concentrating mechanism, in cerebrospinal fluid absorption, and in pulmonary fluid balance.

Several lines of evidence have suggested a relationship between orthogonal arrays of intramembrane particles (OAPs), observed by freeze-fracture electron microscopy, and MIP family members or water channels (Verbavatz et al., 1994). OAPs were identified in lens and shown to consist of MIP protein (Zampighi et al., 1989). OAPs of similar appearance were reported in astroglial cells (Landis and Reese, 1974), gastric parietal cells (Bordi et al., 1986), sarcolemma (Ellisman et al., 1976), kidney collecting duct basolateral membrane (Orci et al., 1981; Nakamura and Nagano, 1985), ciliary epithelium (Hirsch et al., 1988), intestine (Staehelin, 1972; Neutra, 1979), and trachea (Widdicombe et al., 1987), where MIP is absent. Recently, an antibody raised against muscle sarcolemmal vesicles enriched in OAPs was shown to stain kidney collecting duct basolateral membrane and astrocytes (Verbavatz et al., 1994). OAPs have also been associated with the vasopressin-inducible water channel in frog urinary bladder (Chevalier et al., 1974; Brown et al., 1983) and collecting duct apical membrane (Harmanci et al., 1978). The identity and function of OAPs in the basolateral membrane of collecting duct and in non-renal tissues has not been established. CHIP28 also forms characteristic intramembrane particles (IMPs) in native membranes and reconstituted proteoliposomes, although they do not assemble into orthogonal arrays (Verbavatz et al., 1993).

The purpose of this study was to investigate the expression of MIWC and GLIP in non-epithelial tissues and in glandular epithelia not examined in our initial study. Immunogold electron microscopy confirmed the surprising observation by light microscopy that MIWC and GLIP colocalized at the basolateral membrane in kidney collecting duct. Based on northern blot and PCR/Southern blot analyses (Hasegawa et al., 1994; Yang et al., 1995) attention was focused on tissues of the neuromuscular, gastrointestinal and genitourinary systems, and glandular epithelia. MIWC was strongly expressed in the neuromuscular system, at the plasma membrane in astrocytes in brain and spinal cord, and in the sarcolemma of skeletal muscle. In addition, MIWC was expressed on the basolateral membrane of gastric parietal cells and in excretory ducts in salivary and lacrimal glands. Interestingly, this tissue distribution corresponded exactly with the cellular sites in which OAPs have been identified. In contrast, GLIP was not expressed in these tissues, but was found in skin epidermis and transitional epithelium in urinary bladder.

MATERIALS AND METHODS

Immunohistochemistry

Polyclonal antibodies against C terminus synthetic peptides (MIWC, amino acids 287-301, EKGKDSSGEVLSSV; GLIP amino acids 270-285, EAENVKLAHMKHKEQI) were raised in rabbit (MIWC) and mouse (GLIP) as described previously (Frigeri et al., 1995). Antibodies were purified by affinity chromatography (ImmunoPure Ag/Ab purification kit #2, Pierce) according to manufacturer's instructions. Briefly, antibodies were affinity purified utilizing an iodoacetil-crosslinked agarose resin conjugated with each synthetic peptide. Antibodies were eluted at pH 2.5 and pH 11.5, titrated to pH 8, and dialyzed against PBS containing 0.02% sodium azide. There was no cross-reactivity between MIWC and GLIP antibodies.

Rat tissues were perfused with PBS and fixed in situ with PBS containing 4% paraformaldehyde. Organs were removed, sliced and post-fixed for 4 hours, cryoprotected overnight with PBS containing 30% sucrose, embedded in OCT compound, and frozen in liquid N_2. Cryostat sections (4-6 μm) were mounted on Superfrost/Plus microscope slides (Fisher). Slides were incubated for 10 minutes with PBS containing 1% BSA and then with purified MIWC or GLIP antibodies (0.3-0.5 μg/ml) for 1 hour at 23°C in PBS containing 1% BSA. Control experiments were performed using the purified antibodies preadsorbed with excess (>10:1 molar ratio) synthetic peptide. Slides were rinsed with 2.7% NaCl and then with PBS. Antibody-incubated slides were incubated for 30 minutes with peroxidase-conjugated sheep anti-rabbit or mouse $F(ab')_2$ fragment (1:100, Amersham). Peroxidase activity was visualized by reaction with diaminobenzidine (0.5 mg/ml DAB in 0.01 M Tris buffer, pH 7.6, containing 0.3% H_2O_2) for 20 minutes. Slides were counterstained with hematoxylin and photographed using Kodak Gold 100 film on a Nikon Optiphot microscope.

Immunoblot analysis

Organs from Sprague-Dawley rats were removed and homogenized in 200 mM sucrose, 10 mM Tris-HCl, pH 7.4, containing 1 μg/ml leupeptin, 1 μg/ml pepstatin A and 4 μg/ml antipain. After homogenization in a Potter Elvehjem apparatus and centrifugation at 3,000 ***g*** for 10 minutes, a high speed pellet was prepared by centrifugation at 100,000 ***g*** for 60 minutes. Membranes were dissolved in SDS loading buffer, heated to 65°C for 5 minutes, and resolved on a 13% polyacrylamide gel. PVDF membranes containing blotted proteins were blocked with 2% BSA in PBS for 1 hour at room temperature and incubated overnight with immune serum (1:500). Sites of antigen-antibody reaction were visualized by incubation with ^{125}I-Protein A (1 μCi/ml in PBS for 2 hours at 10°C; 1 Ci = 37 GBq) (ICN Biochemicals), followed by 3 washes in PBS and overnight autoradiography at –80°C.

Immunoelectron microscopy

Kidneys from Sprague-Dawley rats were perfused in situ with Hanks' balanced salt solution for 2-3 minutes and then with a fixative containing 3% paraformaldehyde, 0.1% glutaraldehyde, 5% sucrose in PBS for 10 minutes. Organs were removed, sliced, and stored overnight in the same fixative at 4°C, and washed with PBS. Ultrathin frozen sections were prepared and stained using the immunogold procedure as previously described (Tokuyasu, 1986; Verbavatz et al., 1994). Small blocks of fixed kidney tissue were infiltrated with 2.3 M sucrose overnight and frozen in liquid N_2. Sections (60 nm) were cut on a Reichert FC4D ultramicrotome and mounted on carbon/Parlodion-coated copper grids. The grids were preincubated with 0.1% BSA in PBS for 10 minutes, and then incubated with purified MIWC or GLIP antibodies for 60 minutes at 23°C. The grids were washed in PBS, and incubated with Protein A-gold or goat anti-mouse IgG-gold complexes (8 nm gold particles) for 60 minutes. After three washes in PBS, the samples on the grid were further fixed with 1% glutaraldehyde (in PBS) for 5 minutes, washed with water twice for 5 minutes, and stained with 2% uranyl acetate (in water) for 5 minutes. The grids were placed on a drop of 2% methyl cellulose for ~20 seconds, removed with a bacterial wire loop and excess methyl cellulose was blotted. The grids were air dried and viewed on a Philips CM10 electron microscope. This embedding procedure

prevents shrinkage artifacts as the sections dry. For quantification of MIWC and GLIP immunogold labeling, apical and basolateral plasma membranes of collecting duct cells were identified at low magnification on the electron microscope, and higher magnification micrographs (×45,000) were used for counting. The number of gold particles per micron of membrane length was counted from the prints. The length of the membrane was measured by planar morphometry using a graphics tablet interfaced to a Macintosh IIvx computer via a pressure-sensitive pen. The plasma membrane was highlighted with a marker of width of 5-6 gold particle diameters and all particles falling within this line were taken to represent membrane staining. Results were expressed as the number of gold particles per micron of membrane length.

RNase protection assay

RNase protection assays were performed by a modification of the method of Roller et al. (1989). Probes consisted of fragments of rat MIWC (bp 223-579), rat GLIP (bp 208-611) and rat β-actin (bp 2682-2779). The linearized plasmids containing the indicated fragments were transcribed with Sp6 RNA polymerase in the presence of [^{32}P]CTP; 30 μg of total RNA from each tissue was hybridized with the ^{32}P-labeled cRNA probes at 45°C overnight, and then digested with a mixture of RNase A and RNase T1. Protected fragments were resolved on a 5% polyacrylamide-8 M urea gel, blotted onto paper filter and autoradiographed at room temperature overnight. The rat β-actin was used as a control in each lane.

RESULTS

Fig. 1 shows localization of GLIP (Fig. 1A) and MIWC (Fig. 1B) proteins in kidney by immunogold electron microscopy. Specific gold particle labeling was seen at the basolateral plasma membrane of principal cells. In measurements from 10 photographs, the linear density of gold particles (number per μm of membrane) for MIWC immunogold labeling was (mean ± s.e.): 1.59±0.27 (basolateral membrane of principal cells), 0.092±0.032 (apical membrane of principal cells) and 0.082±0.016 (basolateral membrane of intercalated cells). For GLIP immunogold labeling, the corresponding densities were 2.95±0.40, 0.11±0.04 and 0.073±0.03, respectively. Principal cell apical membranes were thus not stained above background levels, and intercalated cells were not stained. No other kidney cell type was stained (not shown). Both antibodies produced a labeling pattern that appeared to lie predominantly on the cystolic side of the plasma membrane, indicating that an internal epitope was labeled. Under the conditions used, staining with GLIP was heavier than that obtained with MIWC antibodies. Double labeling by indirect immunofluorescence of 1 μm sections revealed complete overlap of staining patterns with the two antibodies (not shown). Little or no intracellular labeling was detected, consistent with the constitutive pattern of membrane insertion of these proteins.

Expression of MIWC in brain is shown in Fig. 2. MIWC was not expressed in choroid plexus (Fig. 2A) but was expressed in ependymal cells lining the brain ventricles and aqueductal system (Fig. 2B and C). The low magnification view (Fig. 2B) showed expression also on glial cells at the brain surface. Control slides utilizing a peptide depleted antibody were negative (not shown). A high magnification micrograph of the ependymal cell layer showed strong MIWC expression in ependymal cells without staining of cilia (Fig. 2D). MIWC was observed throughout the brain parenchyma. A section through the third ventricle showed staining of astrocytes in the median eminence of the hypothalamus (Fig. 2E). At higher magnification (Fig. 2F), individual stained astrocyte cell bodies were observed with a plasma membrane staining pattern. The corresponding control slide (Fig. 2H) showed no specific staining. In addition to staining of astrocytes within brain parenchyma, there was also strong staining of astrocyte end-foot processes adjacent to blood vessels (Fig. 2G, see I for control).

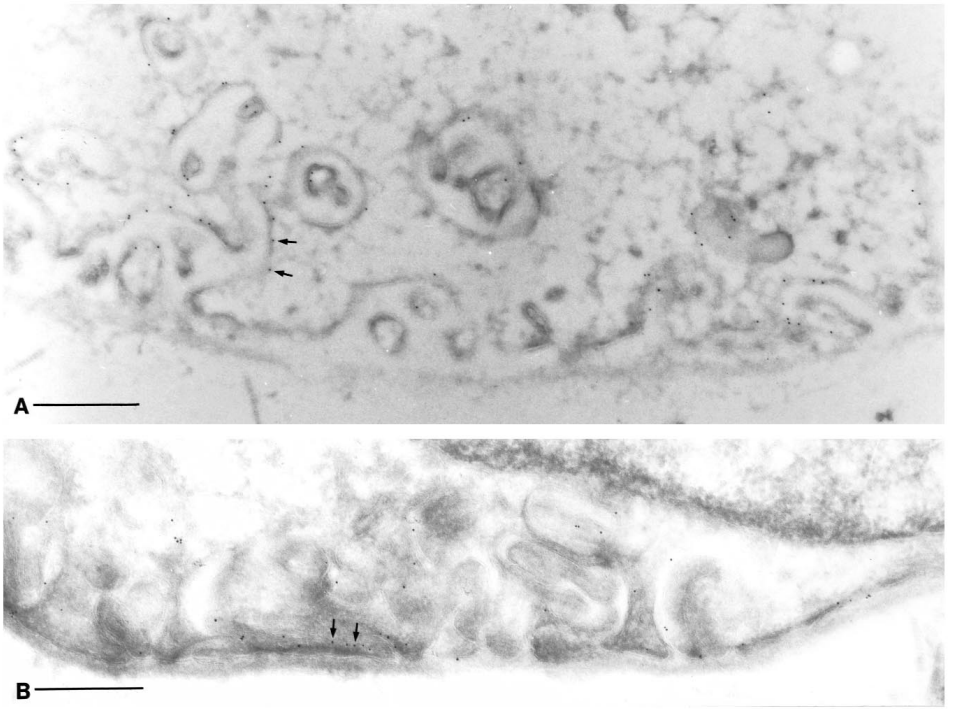

Fig. 1. Immunogold electron microscopy of MIWC and GLIP in kidney papilla. (A) Ultrathin frozen section showing the basolateral plasma membrane domain of a collecting duct principal cell from the inner stripe of rat kidney, stained with anti-GLIP antibodies followed by goat anti-mouse IgG-gold. The gold particle labeling is restricted to the basolateral plasma membrane, and most of the particles are oriented towards the cytoplasmic side of the membrane. No intracellular staining of vesicles is detectable. (B) Staining of a similar section with anti-MIWC antibodies followed by Protein A-gold. Labeling is less intense than with anti-GLIP (A), and often appears as small groups or clusters of particles, whereas the anti-GLIP staining is more evenly distributed along the membrane. Bar, 0.5 μm.

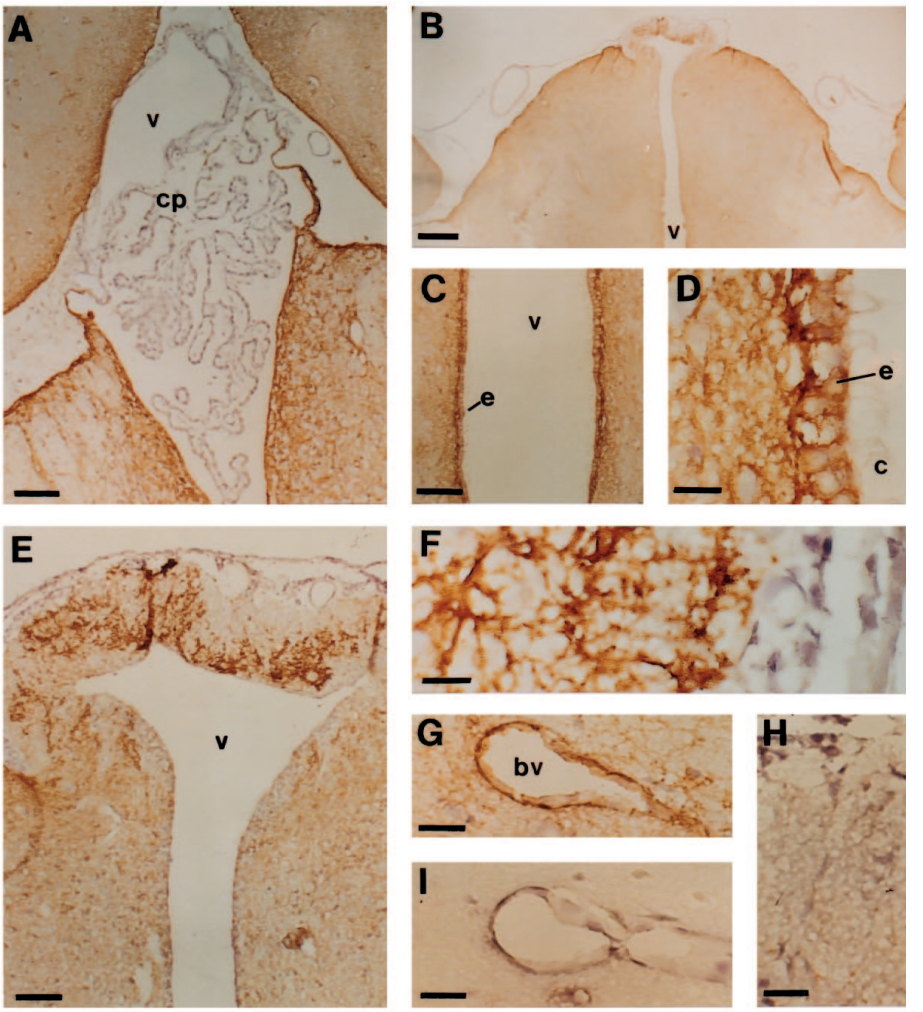

Fig. 2. Localization of MIWC in rat brain. (A) MIWC immunostaining in ependymal cell layer. Note that ependymal cells forming the choroid plexus (cp) are unstained. (B) Low magnification showing the localization on the brain surface. (C) MIWC expression in ependymal cells (e) of the third ventricle (v). (D) High magnification of ependymal cells lining the ventricle with basolateral membrane staining; cilia (c) are unstained. (E) Staining of astrocytes in the ventral portion of the median eminence (me). (F) High magnification of E showing stained astrocytes (a) identified by their star-like shape. (G) Staining of perivascular foot processes of an astrocyte which cover most of the basement membrane of a blood vessel (bv). (H and I) Control sections corresponding to F and G utilizing immunodepleted antibodies. Bars: A,C,E,G,H,I, 70 μm; B, 370 μm; D,F, 12 μm.

MIWC was also expressed in astrocytes throughout the spinal cord (Fig. 3). At low magnification, there was extensive expression throughout the gray matter (Fig. 3A). High magnification of the intermediate zone joining the gray and white matter (Fig. 3B) showed MIWC expression in astrocytes, but not in adjacent neuron cell bodies. High magnification of the white matter (Fig. 3C), which is composed primarily of axons, showed expression of MIWC in astrocytes and their extensions, without expression on axons or neurons. There was no MIWC immunostaining of sciatic nerve (not shown). A control section (Fig. 3D) showing the junction of white and gray matter was negative. As reported previously, GLIP was localized on meningeal cells lining the pia mater (Frigeri et al., 1995), but unlike MIWC, was not found elsewhere in brain parenchyma.

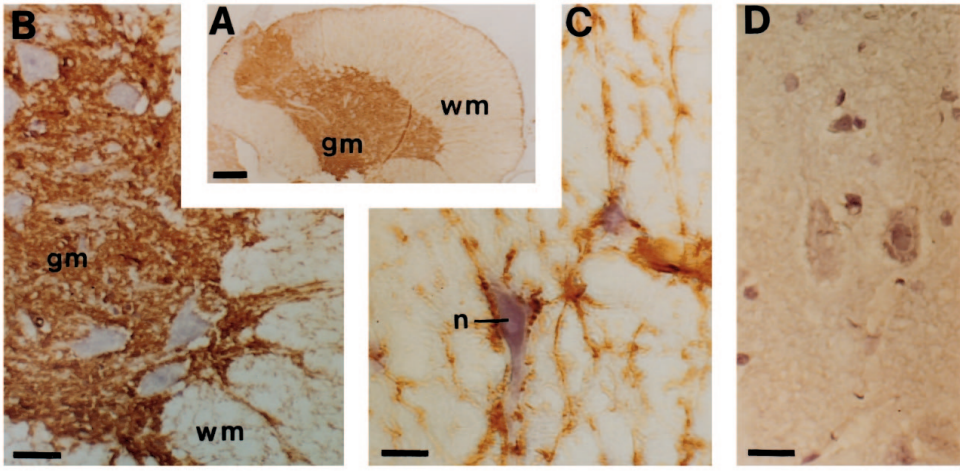

Fig. 3. Localization of MIWC in spinal cord. (A) Low magnification showing dense staining in gray matter (gm). Weaker staining is visible in white matter (wm). (B) High magnification of the gray-white transition zone. The strong staining in the gray matter corresponds to the numerous glial cells whose long and highly branched processes occupy most of the interneuronal space. (C) In white matter, staining was limited to the fibrous astrocytes, and neurons (n) are unstained. (D) Immunodepleted control. Bars: A, 370 μm; B,D, 35 μm; C, 12 μm.

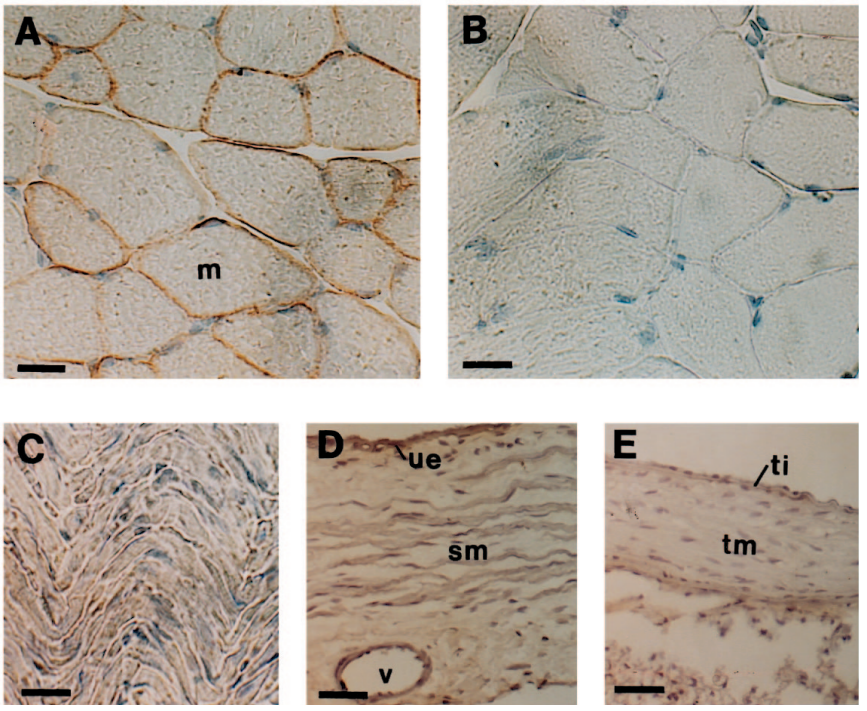

Fig. 4. Expression of MIWC in skeletal muscle. (A) Staining of the sarcolemmal membrane of intercostal muscle. (B) Immunodepleted control. No staining was observed in myocardium (C), urinary bladder smooth muscle (D), or elastic aorta (E). ti, tunica intima; tm, tunica media; ue, urinary epithelium; sm, smooth muscle; v, blood vessel; m, muscle fiber. Bars: A,B,C, 18 μm; D,E, 35 μm.

In muscle, MIWC antibody staining was observed at the sarcolemmal membrane of skeletal muscle (Fig. 4A, see B for control). A similar pattern was found in skeletal muscle from both fast and slow twitch fibers as well as in central and peripheral muscles. In contrast, there was no MIWC antibody staining of cardiac muscle (Fig. 4C) and smooth muscle, as demonstrated in urinary bladder (Fig. 4D) and elastic aorta (Fig. 4E).

In stomach, MIWC was not expressed at the surface epithelium (Fig. 5A), but was found in the parietal cells in oxyntic glands. Deeper layers of the stomach, including smooth muscle, were not labeled. At high magnification (Fig. 5B), MIWC was detected selectively at the basolateral membrane of parietal cells without staining of the apical membrane of parietal cells or membranes in adjacent peptic cells. A control section of stomach (Fig. 5C) was negative. GLIP staining was not observed in any cell type in stomach. However, GLIP immunostaining was found in urinary bladder transitional

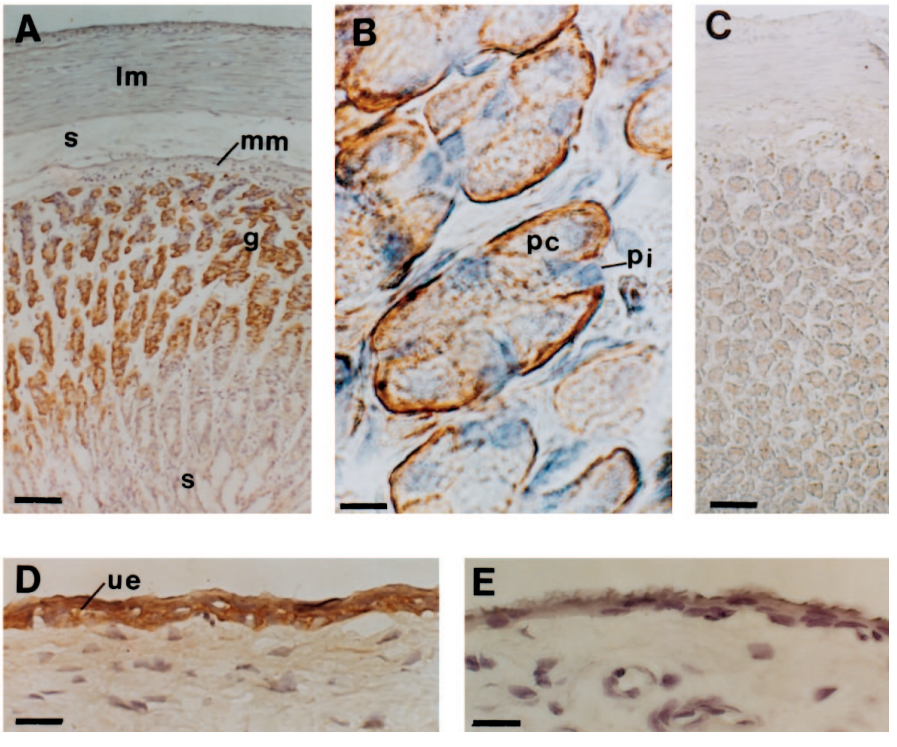

Fig. 5. Immunolocalization of MIWC in stomach and GLIP in urinary bladder. (A) Specific staining in the oxyntic glands (g). No staining was detected on mucosa surface epithelium (se), submucosa (s), longitudinal layer of muscle (lm) or muscularis mucosa (mm). (B) At higher magnification, staining was localized to the basolateral membrane of parietal cells (pc). Note that peptic cells (pi) are unstained. (C) Control section. (D) Localization of GLIP to transitional epithelium in urinary bladder; ue, urinary epithelium. (E) Immunodepleted control. Bars: A,C, 70 μm; D,E, 18 μm; B, 7 μm.

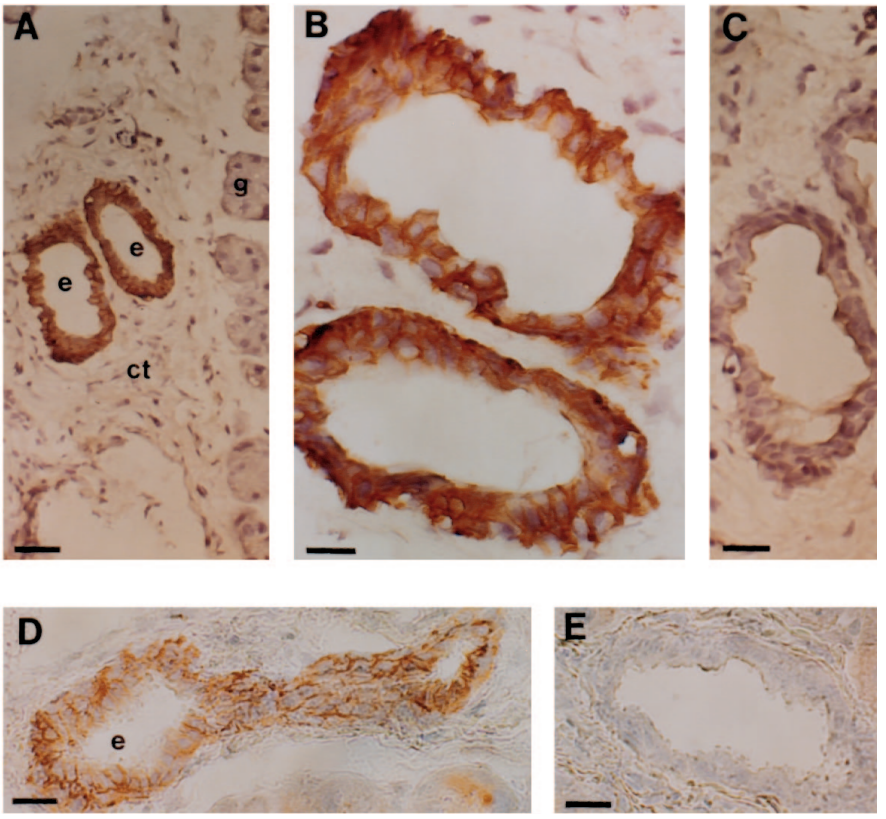

Fig. 6. Immunoperoxidase localization of MIWC in salivary and lacrimal glands. (A) Low magnification showing two excretory ducts (e) labeled in parotid gland. The secretory glands (g) were unstained. (B) High magnification of the two excretory ducts shown in A. The basolateral membrane of the stratified cuboidal epithelium is intensely stained. (C) Immunodepleted control. (D) Excretory duct of an intraorbital lacrimal gland stained with MIWC antibodies showing duct staining. ct, connective tissue. Bars: A, 35 μm; B, 12 μm; C,D,E, 8 μm.

epithelium (Fig. 5D, see E for control), with no staining by MIWC antibody (not shown). Smooth muscle was not labeled by either antibody. Neither MIWC nor GLIP were present in small intestine; however, as reported previously, both proteins were expressed at the basolateral membrane of colonic villus epithelium.

In salivary gland, MIWC was localized to epithelial cells in the excretory duct (Fig. 6A) and not in secretory lobules where a new water channel has been identified recently (Raina et al., 1995). At higher magnification, the basolateral membrane of excretory duct epithelium was primarily stained (Fig. 6B, see C for control). In lacrimal gland, a similar pattern of MIWC localization to the excretory duct was found (Fig. 6D, see E for control). GLIP immunostaining was not detected in these glandular tissues.

Fig. 7 shows strong expression of GLIP in epidermal cells of skin with staining of adjacent sebaceous glands (Fig. 7A, see C for control). At high magnification (Fig. 7B), staining was mainly localized to epidermal cells just beneath the cornified cell layer. MIWC was not found in skin.

The RNase protection assay was used to confirm expression of MIWC and GLIP transcripts in tissues where the proteins were identified by immunostaining (Fig. 8A). The MIWC transcript was strongly expressed in brain, with lesser expression in muscle, kidney, lung and stomach. MIWC expression was absent in liver. Band intensities corresponding to the control probe, β-actin, were similar in each lane. The GLIP transcript was strongly expressed in eye, with lesser expression in bladder, kidney and skin and no expression in liver.

Immunoblot analysis of MIWC is shown in Fig. 8B. A major band of M_r 30 kDa was detected by the MIWC antibody in kidney, stomach and trachea. An additional band of 32 kDa was present in brain homogenate, suggesting that both of the 2 possible translation initiation codons in brain MIWC mRNA are utilized. This finding is consistent with cell-free translation data showing MIWC protein at 30 and 32 kDa (Jung et al., 1994). In contrast, immunoblot of muscle showed a single band at 25-26 kDa and no band at 30 kDa. No bands were observed for liver and heart. Control lanes blotted with pre-immune serum were negative. As reported previously (Frigeri et al., 1995), the 30 kDa band in kidney was absent using preabsorbed antibodies. We were unable to obtain quality immunoblot data for GLIP in tissues other than kidney, which was reported previously.

DISCUSSION

Table 1 summarizes the tissue distributions of MIP family members in mammalian tissues. MIP is expressed only in lens fibers in eye. The vasopressin-inducible water channel (AQP-CD) and an homologous protein (WCH-3; Ma et al., 1993a) are expressed exclusively in kidney. CHIP28, MIWC, GLIP and AQP-5 are expressed is multiple tissues. Except for colocalization of CHIP28 and MIWC in ciliary body in eye, MIWC or GLIP were not detected in cells which express CHIP28. In contrast, MIWC and GLIP colocalized at the same membranes in certain cells of kidney, colon, trachea and brain, but not in others. MIWC, but not GLIP, was expressed in stomach, small airways, astrocytes, and glandular epithelia, whereas GLIP, but not MIWC, was expressed in epidermis and bladder epithelium. As discussed below, the specific tissue distributions

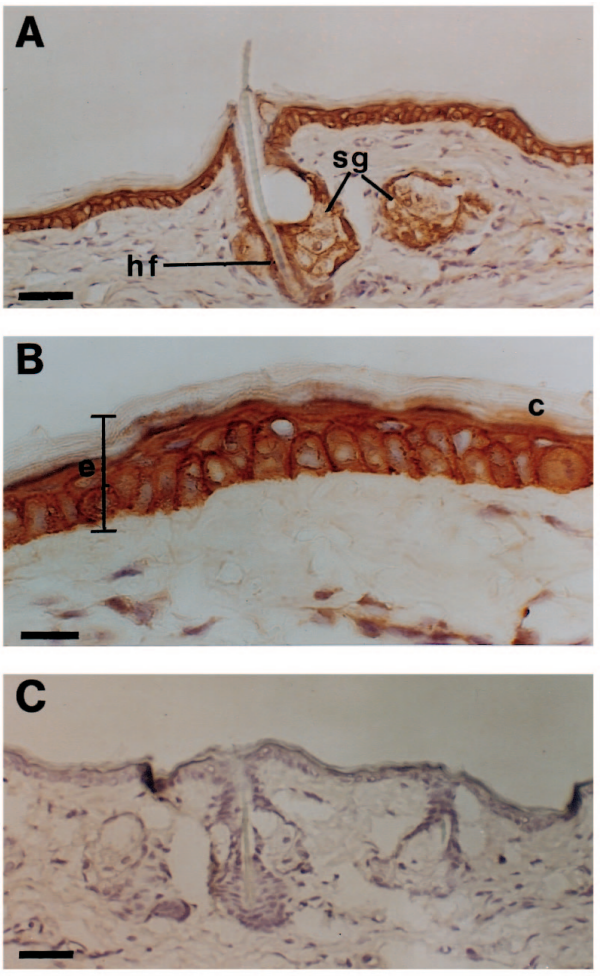

Fig. 7. Expression of GLIP in epidermis. (A) Low magnification of a transverse section of skin showing staining of the entire epidermal layer (e in B). Sebaceous gland (sg) near a hair follicle (hf) are also stained. (B) Higher magnification of epidermis showing a membrane staining pattern. c, cornified layer of the epidermis.
(C) Immunodepleted control. Bars: A,C, 35 μm; B, 12 μm.

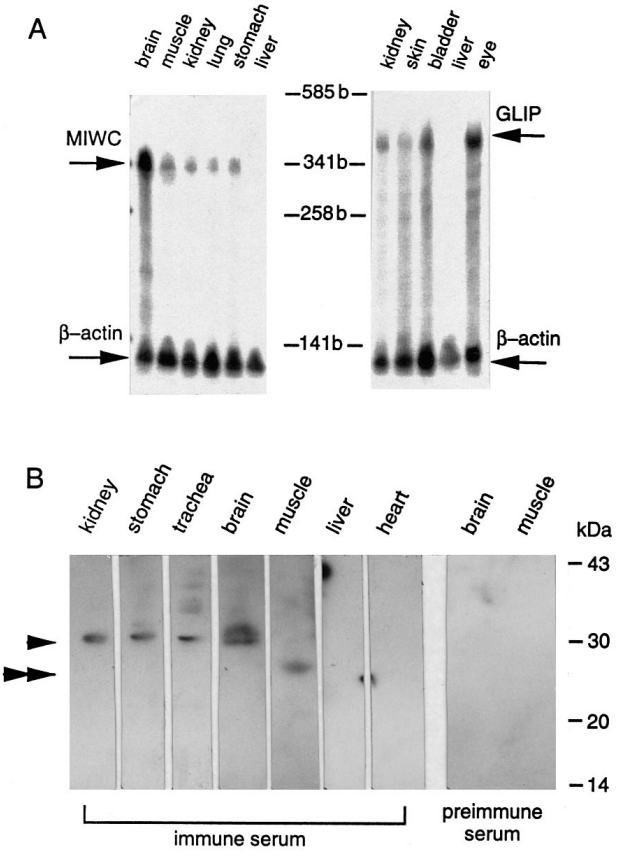

Fig. 8. RNase protection assay and immunoblot analysis of rat tissues. (A) RNase protection assay using probes for MIWC, GLIP and β-actin (see Materials and Methods). Liver is included as a negative control. (B) Immunoblot analysis. Membrane proteins (50 μg/lane) were resolved by SDS-PAGE (12% acrylamide gel) and immunoblotted with anti-MIWC antiserum (first 7 lanes) or pre-immune serum (last 2 lanes at right). Note the 30 kDa band in kidney, stomach and trachea (arrowhead), the two bands in brain, and the 25-26 kDa band in muscle (double arrowhead).

of these proteins suggest participation in transcellular or transmembrane fluid transport.

Of particular interest was the colocalization of MIWC and GLIP at the basolateral membrane of principal cells in kidney collecting duct, demonstrated here by immunogold electron microscopy. This membrane is constitutively water permeable, and contributes to the high transcellular water permeability in collecting duct principal cells after vasopressin stimulation of apical membrane water permeability. The need for 2 different constitutively active water channels in the same membrane, if indeed GLIP functions as a water channel, is unclear: there may be differential regulation of MIWC and GLIP expression and/or function, MIWC and GLIP may serve different functions, or MIWC and GLIP may interact at the molecular level such as in the formation of heterotetramers. The quantitative contributions of MIWC and GLIP to collecting duct water permeability need to be established.

Our initial immunolocalization report demonstrated strong expression of MIWC and GLIP in ependymal cells in the central nervous system (Frigeri et al., 1995). MIWC was found in this study to be expressed throughout the neuromuscular system. MIWC immunostaining was localized to ependymal cells lining the intracerebral ventricles and aqueductal system, and to pia mater, suggesting a role in cerebrospinal fluid reabsorption. The choroid plexus, where cerebrospinal fluid is formed and which contains specialized ependymal cells expressing CHIP28 (Nielsen et al., 1993a; Hasagawa et al., 1994a,b), did not express MIWC. The membranes of astrocytes throughout the brain stained strongly for MIWC. Staining was particularly evident in astrocyte foot processes apposed to pericapillary basement membranes in the median eminence of the hypothalamus. Astrocytes function as structural supportive cells and are thought to be involved in the uptake of chemical transmitters released by neurons and possibly in supplying nutrients to neurons. A recent in situ hybridization study reported MIWC mRNA expression in the area of the supraoptic and paraventricular nuclei of rat brain (Jung et al., 1994); our immunostaining results are in agreement with this finding and show a plasma membrane expression of the MIWC protein. Based on recent physiological studies of mechano-

Table 1. Tissue distribution of MIP family members in rat

Nervous system	
Brain	Choroid plexus: CHIP (e,i); ependymal cells: MIWC (k,u), AQP4* (n)
	Pia mater: MIWC (k,u), GLIP (m)
	Supraoptic and paraventricular nuclei: MIWC (u), AQP4* (n)
	Astrocytes: MIWC (u)
Spinal	Astrocytes: MIWC (u)
Eye	Iris epithelium: CHIP (e,i), MIWC (k); ciliary body: CHIP (e,i), MIWC (k)
	Retina: nuclear layer - MIWC (k, j)
	Cornea: endothelium - CHIP (e,i); epithelium - AQP5* (o)
	Conjuntiva: GLIP (k); lens epithelium: CHIP (e,i); lens fiber: MIP
	Lacrimal gland: excretory duct - MIWC (u); secretory lobule - AQP5* (o)
Musculoskeletal system	
	Skeletal muscle sarcolemma: MIWC (u)
Respiratory system	
	Tracheal epithelium: CHIP* (i), AQP5 * (o), GLIP (k), MIWC (k)
	Bronchial epithelium: MIWC (k); alveolar epithelium: CHIP (p,d*)
Cardiovascular system	
	Myocardium: CHIP (i**, q); capillary endothelium: CHIP (e,i)
Digestive system	
	Salivary gland: excretory duct - MIWC (u) ; secretory lobule - AQP5* (o)
	Stomach: gastric parietal cells - MIWC (u)
	Colon: crypt epithelium - CHIP (e,d); villus epithelium - MIWC (k), GLIP (k)
	Pancreas: CHIP (e); gallbladder CHIP (e,i)
Genitourinary system	
	Kidney WCH-3** (h)
	Proximal tubule and thin descending limb of Henle: CHIP (a,c,d)
	Collecting duct apical membrane: WCH-CD (b)
	Collecting duct basolateral membrane: MIWC (k,u) and GLIP (k,u, l,r*)
	Urinary bladder transitional epithelium - GLIP (u)
Reproductive system	
	Testis efferent ductules, seminal vesicles, prostate: CHIP (f)
	Uterus: CHIP (t); placenta: CHIP (i)
Other	
	Liver: interlobular bile duct - CHIP (e)
	Hematopoietic: spleen red pulp - CHIP (d*,q); erythrocytes - CHIP (s,q)
	Skin: epidermis - GLIP (u); sweat gland - CHIP (i)

*In situ hybridization only; **northern blot analysis only.

References: (a) Sabolic et al., 1992; (b) Fushimi et al., 1993; (c) Nielsen et al., 1993b; (d) Hasegawa et al., 1993; (e) Nielsen et al., 1993a; (f) Brown et al., 1993; (g) Nielsen et al., 1993b; (h) Ma et al., 1993a; (i) Hasegawa et al., 1994a; (j) Hasegawa et al., 1994b; (k) Frigeri et al., 1995; (l) Ishibashi et al., 1994; (m) Ma et al., 1994; (n) Jung et al., 1994; (o) Raina et al., 1995; (p) Folkessen et al., 1994; (q) Bondy et al., 1993; (r) Echevarria et al., 1994; (s) Preston et al., 1991; (t) Li et al., 1994; (u) present paper.

receptor function in superoptic neurons (Oliet and Bourque, 1993), MIWC may also play a role in osmoreceptor function in brain. In spinal cord, MIWC was strongly expressed in astrocytes as observed by diffuse staining of gray matter. Neurons, axon bundles and nerve roots were unstained. Because of the intimate relationship between glial cells and neurons, MIWC may be involved in neuronal support as described above.

We report the first evidence for water channels in skeletal muscle. Initial screening for MIWC in a number of tissues by northern blot showed the highest transcript expression in brain and skeletal muscle (Yang et al., 1995). MIWC transcript expression in skeletal muscle was confirmed by RNase protection assay data in Fig. 8A. By immunostaining, MIWC was expressed on sarcolemmal plasma membranes in skeletal muscle. No immunostaining was observed in cardiac muscle or in smooth muscle from a variety of tissues including urinary bladder, intestine and arteries. Interestingly, immunoblot analysis showed expression of MIWC antibody-reactive proteins at ~30 kDa in brain, kidney, trachea and stomach, but at 25-26 kDa in muscle. Only the 25-26 kDa band was observed in multiple preparations of muscle and in fractionated muscle homogenates. PCR amplification of muscle cDNA (data not shown) with primers flanking the MIWC coding sequence gave a single band with a sequence identical to that reported for MIWC in lung (Hasegawa et al., 1994). It is not known whether the apparently smaller fragment of 25-26 kDa, which should contain the immunoreactive MIWC C terminus, represents translation of a spliced MIWC transcript, a post-translational modification of MIWC, or a closely related protein. The functional role of the various isoforms of MIWC observed in muscle and brain remain unknown.

In the digestive tract, it was reported that MIWC and GLIP are present in the basolateral membrane of colonic villus epithelium (Frigeri et al., 1995). Other gastrointestinal organs were examined here. In salivary gland, MIWC was localized to the excretory duct epithelial layer, but was not seen in glandular cells, where AQP-5 was recently identified (Raina et al., 1995). These findings suggest that water is reabsorbed along the excretory duct to modify the water volume of saliva. A similar staining pattern for MIWC was found in lacrimal gland tissue. In stomach, MIWC localized to the basolateral membrane of parietal cells without apical membrane staining. Studies in isolated membrane vesicles have shown that the apical plasma membrane of gastric parietal cells has low water permeability (Priver et al., 1993). No information is available about the permeability of the contralateral basolateral membrane. If indeed the apical membrane of parietal cells is water-impermeable in vivo, then the presence of a basolateral membrane water channel may be important in cell volume regulation. A water permeable basolateral membrane and impermeable apical membrane would stabilize cell volume and intracellular osmolality during rapid changes in the osmolality of gastric contents.

An unexpected finding was the strong GLIP immunostaining of epidermis and urinary bladder transitional epithelium. Unlike the amphibian urinary bladder, the mammalian bladder is thought to function as a simple storage compartment containing a water-tight epithelium. Chang et al. (1994) recently reported low water permeability in the apical membrane of mammalian bladder epithelium. Similarly, the epidermis has been assumed to serve primarily a barrier function, preventing loss of salt and fluid. Further information about GLIP function(s) is required to address its role in bladder and skin physiology in terms of solute transport or cell volume regulation.

The tissue-specific distribution of MIWC suggests that MIWC may be a principal component of OAPs. Except in lens, where OAPs are comprised of MIP, tissues known to contain OAPs (astrocytes, sarcolemma, trachea, ciliary body, intestine, basolateral membranes of gastric parietal cells, kidney principal cells) were found to express MIWC. It is unclear whether the crystalline arrangement of intramembrane particles in OAPs has any functional significance or whether it is a consequence of the natural tendency of MIP family

members to form 2-dimensional crystals. Definitive identification of MIWC in OAPs will require label-fracture electron microscopy, and determination of whether MIWC can by itself assemble into OAPs will require freeze-fracture studies on proteoliposomes reconstituted with purified MIWC protein.

Supported by grants DK35124, HL42368, HL51854 and DK38452 from the National Institutes of Health, grant R613 from the National Cystic Fibrosis Foundation and a Young Investigator award to M.G. from the Foundation for Anesthesia Education and Research. Dr Frigeri was supported in part by a fellowship from the National Kidney Foundation of California.

REFERENCES

Bondy, C., Chin, E., Smith, B. L., Preston, G. M. and Agre, P. (1993). Developmental gene expression and tissue distribution of the CHIP28 water-channel protein. *Proc. Nat. Acad. Sci. USA* **90**, 4500-4504.

Bordi, C., Amherdt, M. and Perrelet, A. (1986). Orthogonal arrays of particles in the gastric parietal cell of the rat: differences between superficial and basal cells in the gland and after pentagastrin or metiamide treatment. *Anat. Rec.* **215**, 24-34.

Brown, A., Grosso, A. and DeSousa, R. C. (1983). Correlation between water flow and intramembrane particle aggregates in toad epidermis. *Am. J. Physiol.* **245**, C334-C342.

Brown, D., Verbavatz, J. M., Valenti, G., Lui, B. and Sabolic, I. (1993). Localization of CHIP28 water channel in the absorptive segments of the rat male reproductive tract. *Eur. J. Cell Biol.* **61**, 264-273.

Chang, A., Hammond, T. G., Sun, T. T. and Zeidel, M. L. (1994). Permeability properties of the mammalian bladder apical membrane. *Am. J. Physiol.* **275**, C1483-C1492.

Chevalier J., Bourguet J. and Hugon, J. S. (1974). Membrane associated particles: distribution in frog urinary bladder epithelium at rest and after oxytocin treatment. *Cell Tiss. Res.* **152**, 129-140.

Deen, P. M., Verkijk, M. A., Knoers, N. V., Wieringa, B., Monnens, L. A., van Os, C. H. and van Oost, B. A. (1994). Requirement of human renal water channel aquaporin-2 for vasopressin-dependent concentration of urine. *Science* **264**, 92-95.

DiGiovanni, S. R., Nielsen, S., Christensen, E. I. and Knepper, M. A. (1994). Regulation of collecting duct water channel expression by vasopressin in Brattleboro rat. *Proc. Nat. Acad. Sci. USA* **91**, 8984-8988.

Echevarria, M., Windhager, E. E., Tate, S. S. and Frindt, G. (1994). Cloning and expression of AQP3, a water channel from the medullary collecting duct of rat kidney. *Proc. Nat. Acad. Sci. USA* **91**, 10997-11001.

Ellisman, M. H., Rash, J. E., Staehelin, L. A. and Porter, K. R. (1976). Studies of excitable membranes. II. A comparison of specializations at neuromuscular junctions and nonjunctional sarcolemmas of mammalian fast and slow twitch muscle fibers. *J. Cell Biol.* **68**, 752-774.

Folkesson, H. G., Matthay, M. A., Hasegawa, H., Kheradmand, F. and Verkman, A. S. (1994). Transcellular water transport in lung alveolar epithelium through mercurial-sensitive water channels. *Proc. Nat. Acad. Sci. USA* **91**, 4970-4974.

Frigeri, A., Gropper, M., Turck, C. W. and Verkman, A. S. (1995). Immunolocalization of the mercurial insensitive water channel and glycerol intrinsic protein in epithelial cell plasma membranes. *Proc. Nat. Acad. Sci. USA* **92**, 4328-4331.

Fushimi, K., Uchida, S., Hara, Y., Hirata, Y., Marumo, F. and Sasaki, S. (1993). Cloning and expression of apical membrane water channel of rat kidney collecting tubule. *Nature* **361**, 549-552.

Harmanci, M. C., Stern, P., Kachadorian, A., Valtin, H. and DiScala, V. A. (1978). Antidiuretic hormone induced intramembraneous alteration in mammalian collecting ducts. *Am. J. Physiol.* **235**, F440-F443.

Hasegawa, H., Zhang, R., Dohrman, A. and Verkman, A. S. (1993). Tissue-specific expression of mRNA encoding the rat kidney water channel CHIP28k by in situ hybridization. *Am. J. Physiol.* **264**, C237-C245.

Hasegawa, H., Lian, S. C., Finkbeiner, W. E. and Verkman, A. S. (1994a). Extrarenal tissue distribution of CHIP28 water channels by in situ hybridization and antibody staining. *Am. J. Physiol.* **266**, C893-C903.

Hasegawa, H., Ma, T., Skach, W., Matthay, M. and Verkman, A. S. (1994b). Molecular cloning of a mercurial-insensitive water channel expressed in selected water transporting tissues. *J. Biol. Chem.* **269**, 5497-5500.

Hirsch, M., Gache, D. and Noske, W. (1988). Orthogonal arrays of particles in non-pigmented cells of rat ciliary epithelium: relation to distribution of filipin and digitonin-induced alterations of the basolateral membrane. *Cell Tissue Res.* **252**, 165-173.

Ishibashi, K., Sasaki, S., Fushimi, K., Uchida, S., Kuwahara, M., Saito, H., Furukawa, T., Nakajima, K., Yamaguchi, Y., Gojobori, T. and Marumo, F. (1994). Molecular cloning and expression of a member of the aquaporin family with permeability to glycerol and urea in addition to water expressed at the basolateral membrane of kidney collecting duct cells. *Proc. Nat. Acad. Sci. USA* **91**, 6269-6273.

Jung, J. S., Bhat, R. V., Preston, G. M., Guggino, W. B., Baraban, J. M. and Agre, P. (1994). Molecular characterization of an aquaporin cDNA from brain: candidate osmoreceptor and regulation of water balance. *Proc. Nat. Acad. Sci. USA* **91**, 13052-13056.

Landis, D. M. D. and Reese, T. S. (1974). Arrays of particles in freeze-fractured astrocytic membranes. *J. Cell Biol.* **60**, 316-320.

Li, X., Yu, H. and Koide, S. S. (1994). The water channel gene in human uterus. *Biochem. Mol. Biol. Int.* **32**, 371-377.

Ma, T., Frigeri, A., Skach, W. and Verkman, A. S. (1993a). Cloning of a cDNA from rat kidney with homology to CHIP28 and WCH-CD water channels. *Biochim. Biophys. Res. Commun.* **197,** 654-659.

Ma, T., Frigeri, A., Tsai, S. T., Verbavatz, J. M. and Verkman, A. S. (1993b). Localization and functional analysis of CHIP28k water channels in stably transfected CHO cells. *J. Biol. Chem.* **268,** 22756-22764.

Ma, T., Frigeri, A., Hasegawa, H. and Verkman, A. S. (1994). Cloning of a water channel homolog expressed in brain meningeal cells and kidney collecting duct that functions as a stilbene-sensitive glycerol transporter. *J. Biol. Chem.* **269**, 21845-21849.

Nakamura, T. and Nagano, T. (1985). Intramembrane particle distribution in renal collecting tubule cells in normal, dehydrated and hereditary diabetes insipidus rats with particular reference to orthogonal arrays of particles. *J. Electron Microsc. (Tokyo)* **34**, 364-372.

Neutra, M. R. (1979). Linear arrays of intramembrane particles on microvilli in primate large intestine. *Anat. Rec.* **193**, 367-382.

Nielsen, S., Smith, B. L., Christensen, E. I. and Agre, P. (1993a). Distribution of the aquaporin CHIP in secretory and resorptive epithelia and capillary endothelia. *Proc. Nat. Acad. Sci. USA* **90**, 7275-7279.

Nielsen, S., Smith, B. L., Christensen, E. I., Knepper, M. A. and Agre, P. (1993b). CHIP28 water channels are localized in constitutively water-permeable segments of the nephron. *J. Cell Biol.* **120**, 371-383.

Oliet, S. H. and Bourque, C. W. (1993). Mechanosensitive channels transduce osmosensitivity in supraoptic neurons. *Nature* **364**, 341-343.

Orci, L., Humbert, F., Brown, D. and Perrelet, A. (1981). Membrane ultrastructure in urinary tubules. *Int. Rev. Cytol.* **73**, 183-242.

Preston, G. M. and Agre, P. (1991). Isolation of the cDNA for erythrocyte integral membrane protein of 28 kilodaltons: member of an ancient channel family. *Proc. Nat. Acad. Sci. USA* **88,** 11110-11114.

Preston, G. M., Carroll, T. P., Guggino, W. B. and Agre, P. (1992). Appearance of water channels in *Xenopus* oocytes expressing red cell CHIP28 protein. *Science* **256**, 385-387.

Priver, N. A., Rabon, E. C. and Zeidel, M. L. (1993). Apical membrane of the gastric parietal cell: water, proton, and nonelectrolyte permeabilities. *Biochemistry* **32**, 2459-2468.

Raina, S., Preston, G. M., Guggino, W. B. and Agre, P. (1995). Molecular cloning and characterization of an aquaporin cDNA from salivary, lacrimal, and respiratory tissues. *J. Biol. Chem.* **270**, 1908-1912.

Reizer, J., Reizer, A. and Saier, M. H. (1993). The MIP family of integral membrane channel proteins: sequence comparisons, evolutional relationships, reconstructed pathway of evolution, and proposed functional differentiation of two repeated halves of the protein. *Crit. Rev. Biochem. Mol. Biol.* **28**, 235-257.

Roller, R. J., Kinloch, R. A., Hiraoka, B. Y., Le, S. S.-L. and Wassarman, P. M. (1989). Gene expression during mammalian oogenesis and early embryogenesis: quantification of three messenger RNAs abundant in fully grown mouse oocytes. *Development* **106**, 251-261.

Sabolic, I., Valenti, G., Verbavatz, J. M., Van Hoek, A. N., Verkman, A. S., Ausiello, D. A. and Brown, D. (1992). Localization of the CHIP28 water channel in rat kidney. *Am. J. Physiol.* **263**, C1225-C1233.

Sabolic, I., Katsura, T., Verbavatz, J. M. and Brown, D. (1995). The AQP2 water channel: effect of vasopressin treatment, microtubule disruption, and distribution in neonatal rats. *J. Membr. Biol.* **143**, 165-175.

Staehelin, L. A. (1972). Three types of gap junctions interconnecting intestinal

epithelial cells visualized by freeze etching. *Proc. Nat. Acad. Sci. USA* **69**, 1318-1321.

Tokuyasu, K. T. (1986). Application of the cryoultramicrotomy to immunocytochemistry. *J. Microsc.* **143**, 139-149.

Van Hoek, A. N. and Verkman, A. S. (1992). Functional reconstitution of the isolated erythrocyte water channel CHIP28. *J. Biol. Chem.* **267**, 18267-18269.

Verbavatz, J. M., Brown, D., Sabolic, I., Valenti, G., Ausiello, D. A., Van Hoek, A. N., Ma, T. and Verkman, A. S. (1993). Tetrameric assembly of CHIP28 water channels in liposomes and cell membranes. A freeze-fracture study. *J. Cell Biol.* **123**, 605-618.

Verbavatz, J. M., Van Hoek, A. N., Ma, T., Sabolic, I., Valenti, G., Ellisman, M., Ausiello, D. A., Verkman, A. S. and Brown, D. (1994). A 28 kD sarcolemmal antigen in kidney principal cell basolateral membranes: relationship to orthogonal arrays and MIP26. *J. Cell Sci.* **107**, 1083-1094.

Verkman, A. S. (1993). *Water Channels*. R. G. Landes Company, Austin, Texas.

Widdicombe, J. H., Coleman, D. L., Finkbeiner, W. E. and Friend, D. S. (1987). Primary cultures of the dog's tracheal epithelium: fine structure, fluid, and electrolyte transport. *Cell Tissue Res.* **247**, 95-103.

Yang, B., Ma, T. and Verkman, A. S. (1995). Genomic organization of the human mercurial-insensitive water channel. *J. Biol. Chem.* (in press).

Zampighi, G. A., Hall, J. E., Ehring, G. R. and Simon, S. A. (1989). The structural organization and protein composition of lens fiber junctions. *J. Cell Biol.* **108**, 2255-2275.

Zhang, R., Skach, W., Hasegawa, H., Van Hoek, A. N. and Verkman, A. S. (1993). Cloning, functional analysis and cell localization of a kidney proximal tubule water transporter homologous to CHIP28. *J. Cell Biol.* **120**, 359-369.

(Received 15 March 1995 - Accepted 21 June 1995)